# FACET TOLERANCES FOR STATIC AND DYNAMIC MISALIGNMENT*

J. Frederico, M. J. Hogan, T. Raubenheimer,
SLAC National Accelerator Laboratory, Menlo Park, CA 94025

## Abstract

The Facility for Advanced Accelerator and Experimental Tests (FACET) at the SLAC National Accelerator Laboratory is designed to deliver a beam with a transverse spot size on the order of 10 $\mu$m $\times$ 10 $\mu$m in a new beamline constructed at the two kilometer point of the SLAC linac. Commissioning the beamline requires mitigating alignment errors and their effects, which can be significant and result in spot sizes orders of magnitude larger. Sextupole and quadrupole alignment errors in particular can introduce errors in focusing, steering, and dispersion which can result in spot size growth, beta mismatch, and waist movement. Alignment errors due to static misalignments, mechanical jitter, energy jitter, and other physical processes can be analyzed to determine the level of accuracy and precision that the beamline requires. It is important to recognize these effects and their tolerances in order to deliver a beam as designed.

# INTRODUCTION

## FACET Design

The Facility for Advanced Accelerator and Experimental Tests (FACET) at the SLAC National Accelerator Laboratory is designed to deliver a beam with a transverse spot size on the order of 10 $\mu$m $\times$ 10 $\mu$m, with 3.2 nC charge at 20 GeV. One of several applications of the FACET beam will be beam-driven plasma wakefield acceleration (PWFA). In beam-driven PWFA at FACET, focused electron beams are passed through a lithium vapor, ionizing the lithium. The high-charge beam drives the plasma electrons out in a blowout regime bubble, which collapses to form accelerating gradients on the order of tens of GeV/m [1].

## Parameters Affecting User Experiments

In order for users to perform a successful experiment, several conditions must be met. Plasma wakefield acceleration requires high fields generated by tightly-focused beams in order to ionize the plasma and create a bubble. Once focused, other parameters such as emittance and dispersion become important. Emittance determines the divergence rate of the focused beam and the length of the interaction [3], while dispersion coupled with energy spread can produce tilted beams that may excite the two-stream hosing instability [4].

Table 1: Typical Operating Parameters for the FACET Beamline

| Simulated FACET Parameters [2] | |
|---|---|
| Energy | 20 GeV |
| RMS Energy Spread | 1.5% |
| Species | electrons |
| Charge per bunch | 3.2 nC |
| Transverse spot size (IP) | 10 $\mu$m $\times$ 10 $\mu$m |
| Bunch length | 20 $\mu$m |
| Plasma Type | lithium |
| Plasma Density | $10^{16}$ - $3 \times 10^{17}$ e$^-$/cm$^3$ |
| Sec. 20 Entrance Norm. $\epsilon_x$ | 90.0 mm-mrad |
| Sec. 20 Entrance Norm. $\epsilon_y$ | 4.09 mm-mrad |

Longitudinal bunch length is also a factor in PWFA, as well as several other user experiments, including Smith-Purcell radiation [5]. In PWFA in particular, shorter bunches drive larger and more well-defined wakes, resulting in higher acceleration gradients.

## Understanding and Correcting Misalignments

In order to obtain bounds on alignment errors, optics errors introduced by individual elements must be understood. Optics errors may occur for a variety of reasons. Power-supply errors change magnetic fields in optics magnets, which changes focusing and chromatic cancellation. Mechanical offsets, both jitter and static, can occur due to vibration, thermal fluctuations, and the limitations of alignment measurements. Energy jitter can occur as well resulting from RF jitter and wakefields.

**Quadrupole Misalignments** Beam offsets in quadrupoles introduce dipole fields. This combined-function quadrupole-dipole field generates trajectory error as well as dispersion on top of pre-existing dispersion evolution within the quadrupole. Uncorrected dispersion of this type is the primary cause of spot size growth at the IP for this type of error.

The dispersion equation to lowest order in $\delta$, with a bend radius of $\rho$, is given by [6]: $D'' + \left(1/\rho^2 + k\right) D = 1/\rho$. In terms of geometric focusing strength $K_1$ and a small offset $\Delta x$, recognizing that an offset in a quad leads to a bend radius $1/\rho = |K_1|\Delta x$, dispersion solutions for a combined-
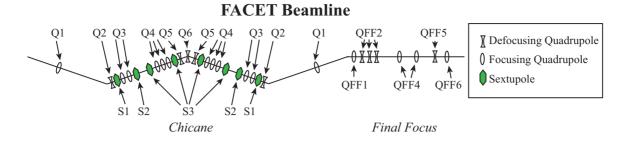
## FACET Beamline



Figure 1: The FACET beamline, showing quadrupoles and sextupoles.

function quadrupole are given by [6]:

$$\Delta\eta(s) = \begin{cases} \dfrac{K_1 \Delta x}{K}\left[1 - \cos\left(\sqrt{K}s\right)\right] & \text{if } K > 0 \\[2ex] \dfrac{K_1 \Delta x}{|K|}\left[-1 + \cosh\left(\sqrt{|K|}s\right)\right] & \text{if } K < 0 \end{cases} \quad (1)$$

where $K = k^2 \Delta x^2 + K_1$. To first order in $\Delta x$, $K \approx K_1$, and can be approximated as such.

Dispersion errors are expected to be the highest-order contributions of offsets in quads. With a particle's $x$-coordinate given by $x_2 = R_{11}x_1 + R_{12}x_1' + \eta\delta_1$, spot size becomes

$$\langle \sigma_{\text{RMS}}^2 \rangle = \sigma_{0,\,\text{RMS}}^2 + \langle \Delta\eta^2 \rangle \sigma_{\delta,\,\text{RMS}}^2$$

$$\Rightarrow \langle \Delta\sigma_{\text{RMS}} \rangle \approx \frac{\sigma_{\delta,\,\text{RMS}}^2}{2\sigma_{0,\,\text{RMS}}}\langle (\Delta\eta_{IP})^2 \rangle \quad (2)$$

The sensitivity to misalignment can be found by pulling out the $\sigma_{\Delta x}$ factor from $\langle (\Delta\eta_{IP})^2 \rangle$ in Eq. 2.

**Sextupole Misalignments** Offsets in a sextupole produce quadrupole fields for $x$ offsets and skew quadrupole fields for $y$ offsets. Quadrupole fields are small: $K_{1,\,eff} = -K_2 \Delta q$ where $q$ is the offset. Weak $K_{1,eff}$ fields imply the dispersion does not change significantly over the length of the effective quadrupole. The dispersion equation can then be integrated to find the error introduced to $\eta'$, while errors in $\eta$ are higher order in $L$:

$$D' = \int_0^L (D'' = -kD)\, \mathrm{d}l$$

$$\Rightarrow \Delta\eta_{[x/y],\,IP} = -R_{[12/34]}\eta_{0,\,[x/y]}LK_2\Delta x \quad \text{for } \Delta x \quad (3)$$

$$\Rightarrow \Delta\eta_{[x/y],\,IP} = -R_{[12/34]}\eta_{0,\,[y/x]}LK_2\Delta y \quad \text{for } \Delta y \quad (4)$$

The dispersion errors are the dominant form of errors in the FACET sextupoles. The sextupoles are designed to correct chromatic aberrations, and are at points of large dispersion; focusing errors due to quadrupole fields are secondary. Dispersion errors contribute to spot size as mentioned previously in Eq. 2.

## SIMULATION SETUP

100-sample Monte Carlo Elegant simulations were performed and compared to baseline simulations to determine
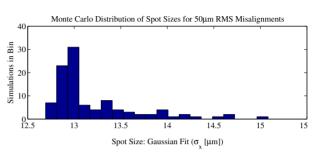


Figure 2: Distribution of spot sizes for 100 Monte Carlo simulations of a Gaussian misalignment in $x$ with $\sigma_{\Delta x} = 50\ \mu$m.

error growth due to jitter. Due to computational limitations, beam steering was not performed. These simulations are expected to show larger spot size growth than the analytic calculations, as an offset introduced in a quadrupole will create steering and effectively misalign all of the downstream elements which will produce further dispersion contributions. This is not consistent with a static misalignment that can and will be steered for in a physical experiment. However, it is useful to determine an upper bounds on acceptable mechanical jitter, as well as an upper bounds on spot size growth with steering applied to correct misalignments.

Spot sizes and dispersion at the IP are already tuned to be minima. A typical spot size distribution including jitter error is a chi-squared distribution as in Fig. 2. However, the mean of this distribution - the average spot size - is the figure of merit, and the sensitivity of the average spot size to amount of jitter was calculated.
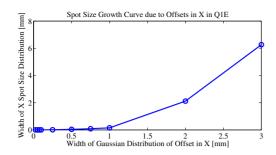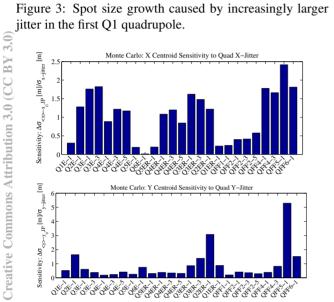
## RESULTS

Results of simulations can be found in Figs. 4-6. Quadrupoles within the chicane are more sensitive than quads throughout the rest of the linac. Two clear families of quadrupoles drive spot size growth: Q2, Q3, and Q4 families in $x$; and Q2, Q3, and Q6 families in $y$. The final focus optics does not affect spot size as strongly as the chicane. The same quadrupole families are also relatively sensitive in driving steering errors, with the addition of several final focus quads (Fig. 4).

The Monte Carlo simulation results for sextupoles show

Figure 3: Spot size growth caused by increasingly larger jitter in the first Q1 quadrupole.
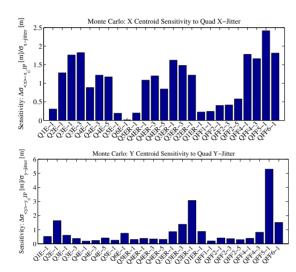


Figure 4: Quadrupole steering jitter is decoupled between planes. Offsets in quadrupoles generate angular kicks that propagate to the IP.

that the S2 family is far more sensitive than the rest. Strong $x$ dispersion at the sextupoles couples into the $y$ plane where $y$ jitter creates skew quadrupole fields. The sensitivity of the S2 sextupoles has been observed in machine commissioning.

## CONCLUSIONS

It is possible to determine which quadrupoles are more sensitive to jitter error. Further work should expand the analysis to include static misalignment error and the steering that is required. Misalignment analysis has laid the groundwork for analysis of other sources of error. Element rolls, power supply jitter and error, and beam energy jitter and error can be analyzed with the same simulation code.

In particular, it will be of interest to determine the sensitivity of quadrupole misalignments that have been corrected. In this case, steering will make IP dispersion and spot sizes less sensitive to errors. However, if steering cannot correct for misalignments at a tolerable level, other solutions may need to be investigated. It is possible more sensitive quads may need more thorough alignment, or possibly movers capable of micron-level alignment.
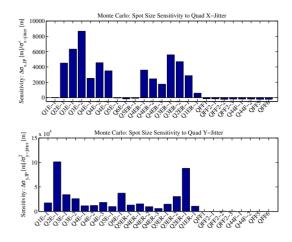


Figure 5: Quadrupole jitter drives spot size growth for quadrupoles within the chicane. In particular: the Q2, Q3, and Q4 quadrupole families are sensitive in $x$, while the Q2, Q3, and Q6 quadrupoles are most sensitive in $y$.
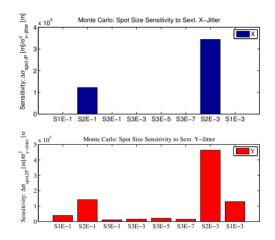


Figure 6: Sextupole jitter contributions to beamsize growth was difficult to observe in simulation. Growth from S2 sextupoles was the only apparent contribution above noise for $x$-jitter. $Y$-jitter only contributed significantly to $y$-growth.

## REFERENCES

[1] M. J. Hogan et al., Plasma Wakefield Acceleration Experiments at FACET, New Journal of Physics, 12 (2010).

[2] M. J. Hogan et al., Plasma Wakefield Experiments at FACET, in PAC Conf. '11, New York, NY, Mar. 2011.

[3] I. Blumenfeld et al., Energy Doubling of 42 GeV Electrons in a Metre-Scale Plasma Wakefield Accelerator, Nature 445 (2007) 7129.

[4] C. Huang et al., Hosing Instability in the Blow-Out Regime for Plasma-Wakefield Acceleration, Physical Review Letters 99 (2007) 25.

[5] N. Delerue et al., Electron Bunch Profile Diagnostics in the Few fs Regime using Coherent Smith-Purcell Radiation, in IPAC 2011, 2011.

[6] S.-Y. Lee, *Accelerator Physics*, World Scientific Publishing Co. Pte. Ltd., Hackensack, NJ, 2004.